ASSESSMENT AND APPLICATION OF A SINGLE-CHARGE BLAST TEST AT THE KIRUNA MINE, SWEDEN

D.R. Tesarik[1], W.A. Hustrulid[2] & U. Nyberg[3]

[1, 2] NIOSH, Office of Mine Safety and Health Research, 315 E. Montgomery Ave, Spokane, WA 99207;
[1]D.R. Tesarik, det4@cdc.gov; [2]W.A. Hustrulid, bet1@cdc.gov
[3] Division of Mining and Geotechnical Engineering, Luleå University of Technology, SE-971 87 Luleå, Sweden; ulf.nyberg@ltu.se

ABSTRACT

Peak particle velocity (PPV) and distance measurements from a single-charge blast test conducted by Swedish researchers in iron ore at the Kiruna Mine in northern Sweden are presented. They are used along with theoretical PPVs calculated using an equation based on hydrodynamics to determine a damage distance range caused by a single charge. This equation, which relates PPV to explosive properties, charge geometry, and distance from a charge, was then applied to a charge of different geometry that was used in drift rounds. A comparison between calculated and measured PPVs suggests that the stoping holes likely damage the easer hole locations, and the easer holes produce damage to the perimeter hole locations. The practical effect is that typical damage limit predictions based on measurements conducted in fresh or undamaged rock are conservative. This suggests that even when perimeter control is not exercised in drifting (i.e., the perimeter holes are fully loaded), the resulting damage may be less than normally expected due to the wave damping effect of the pre-damaged rock. Due to the damping effect, poor perimeter blasting practices are somewhat self correcting. However, it must be strongly emphasized that well-engineered blast designs with perimeter control are highly beneficial in relation to both economic and safety aspects.

1. INTRODUCTION

Blast damage around excavation perimeters is a contributing factor to injuries caused by rockfalls in underground mines. This unwanted perimeter damage also results in extra time required to scale and install supports under potentially hazardous ground conditions. By implementing controlled blasting, perimeter damage can be minimized and underground safety improved. Methods, such as line drilling, presplitting, cushion blasting, fracture control blasting, and smooth blasting are successfully used in civil tunneling operations (Lizotte 1994, Olofsson 1990); but, they are less often used in the mining industry because of perceived additional costs and the expected life of underground openings is generally much less than that of civil structures. However, when carefully looking at the complete cost/benefit picture regarding perimeter control blasting in drift driving, it is clear that the contribution of perimeter control is economically desirable (Miller & Camm 2009). Additional drilling and blasting costs are balanced by reduced dilution, less scaling time and support requirements, less ground rehabilitation costs, and other items. An additional benefit of prime concern to the National Institute for

Occupational Safety and Health (NIOSH) is the increase in personnel safety achieved by reducing exposure to loose material in the perimeter of a mine opening.

A commonly applied approach for perimeter control blast design was developed by Holmberg and Persson (1979). It is based on the peak particle velocity (PPV) generated at a certain distance away from a charge of known explosive weight. The limiting PPV value is the velocity associated with the extent of the damage zone. In practice, the damage zone limit is identified by various methods including visual, shear or p-wave velocity measurements, core strength determinations as a function of distance away from the blasthole, and other methods (Iverson et al. 2009). Several other perimeter blast design approaches use PPV as a measure of damage. These include work by Hustrulid et al. (1992), who developed a PPV dampening law based on the calculated pressure in the blasthole, and Blair and Minchinton (2006), who developed the Scaled Heelen model which uses linear waveform superposition to calculate particle velocity at a given point. Blair also used nonlinear superposition to calculate blast vibration for both single charges and full-scale blasts (Blair 2008). Neiman and other Russian researchers applied hydrodynamic theory to develop a relationship between PPV, rock and explosive parameters, and charge geometry (Neiman 1976, 1979, 1984a, 1984b, 1986a, 1986b). A summary of their work is presented by Hustrulid (1999).

This paper uses equations developed by Neiman as well as PPV and distance measurements collected by Swedish researchers (Nyberg 1998, Jinnerot and Nilsson 1998) to analyze damage around individual charges. The field tests were conducted jointly by the Swedish Rock Research Foundation (SveBeFo) and Luossavaara-Kiirunavaara Aktiebolaget (LKAB) at LKAB's Kiruna Mine in Northern Sweden. The overall objective of the field study was to develop a basis for more effective drift driving in varying geological conditions. The immediate aim was to reduce damage to the perimeter and overbreak and, consequently, reduce scaling and reinforcement requirements.

2. KIRUNA MINE

LKAB's Kiruna Mine is located in the rich iron ore fields of northern Sweden. LKAB started mining the fine-grained magnetite ore in the late 1800s using open pit methods and switched to underground methods in the 1950s. Today, the primary method of mining is sublevel caving (Lupo 1997).

The ore body is approximately 4 km long with an average width of 85 m and an estimated depth of 2 km. It dips at about 60^{o} to the east and plunges to the north. The main level lies 1,045 m below the surface and mining takes place between the 775- and 1,045-m levels. The mine produces about 26 million tons of crude ore per year (www.LKAB.com 2010).

The footwall consists of either trachite or rhyolite with layers of trachite. The rock in the hanging wall is rhyodacite with dikes of diabase and porphyry. The shears in the ore body are filled with calcite or pyrite. The joints are tight but numerous, sometimes

having a thin hematite coating. Some crushing and clay alteration has been encountered in core recovered from diamond drill holes (Nyberg et al. 1998). Material properties for the magnetite are listed in Table I.

Material Property	**Value**
Compressive strength	115 MPa
Density	4,800 kg/m^3
Seismic velocity, across drifts (N-S)	4,880 m/s
Seismic velocity, along drifts (E-W)	6,273 m/s

Table I- Material properties for the Kiruna ore (Nyberg et al. 1998)

3. VELOCITY EQUATIONS FOR A CYLINDRICAL CHARGE

3.1 Theoretical background

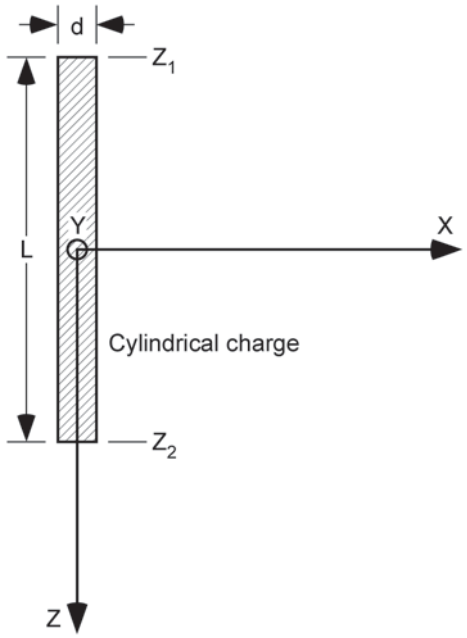

Figure 1- Cylindrical charge with coordinate axes origin at centroid of charge.

Neiman (1976, 1979, 1984a, 1984b, 1986a, 1986b) used hydrodynamic principles to develop equations (1 – 3) that express the velocity components at a given location from a detonating cylindrical charge as a function of specific density of the explosive, energy per unit mass of the explosive, specific density of the rock, geometry of the charge and the three Cartesian coordinates at the specified location from the charge. Figure 1 shows a diagrammatic representation of the geometry to be used (Hustrulid 1999).

$$V_x = Px(AB - CD) \quad (1)$$

$$V_y = Py(AB - CD) \quad (2)$$

$$V = Pz(C - A) \quad (3)$$

where:

$$A = \frac{1}{\sqrt{x^2 + y^2 \quad (z_1 - z)^2}} \quad (4)$$

$$B = \frac{1}{{}_1 - z + \sqrt{x^2 + y^2 \quad (z_1 - z)^2}} \quad (5)$$

$$C = \frac{1}{\sqrt{x^2 + y^2 \quad (z_2 - z)^2}} \quad (6)$$

$$D = \frac{1}{z_2 - z + \sqrt{x^2 + y^2 \quad (z_2 - z)^2}} \quad (7)$$

$$P = d\sqrt{\frac{\rho_e q_e}{8\rho_r v_s}} \quad (8)$$

ρ_e = density of the explosive
q_e =specific energy of the explosive
ρ_r =density of the rock
z_1, z_2 = z coordinates at charge ends
x, y, z = coordinates of the point in question

$$v_s = \ln\left(\frac{\bar{L} \quad \sqrt{\quad \bar{L}}}{-\bar{L}y \quad \sqrt{y \quad \bar{L}}}\right) \quad (9)$$

$$\bar{L} = \frac{L}{d} \quad (10)$$

d = hole diameter
L = charge length

The PPV is defined as

$$PPV = \sqrt{V_x{}^2 + V^{\,2} + V^{\,2}} \quad (11)$$

Equation (12) is the expression for the theoretical radial velocity, u_t, along the x axis for a cylindrical charge of length L and diameter d:

$$u_t = I \; \mathrm{G_t}^{-1} \quad (12)$$

where

$$I = \sqrt{\frac{\rho_e q_e}{8\rho_r}} \tag{13}$$

$$G_t = \frac{\sqrt{v_s}\,\bar{r}\sqrt{\bar{r}^2 + \frac{\bar{L}^2}{4}}}{\bar{L}} \tag{14}$$

r = the distance along the x axis.

$$\bar{r} = \frac{r}{d}$$

The explosive parameters are contained in the multiplying constant I. The charge geometric terms are contained in the parameter G_t. Neiman used the symbol ρ to represent this parameter (Hustrulid 1999). It has been changed to G_t in this paper to avoid confusion with the symbol ρ used in conjunction with rock and explosive density.

Neiman (1979) has shown that the equation for measured radial velocity, u_f, from field tests has the same form as equation (12) where I_f and α are determined from measured data:

$$u_f = {}_f G_t^{-\alpha} \tag{15}$$

Equation (15) can be used to assess the extent of damage from single charges if the critical PPV and the values of I_f and α have been determined by field measurements. In general, measured PPVs are less than theoretical PPVs because of discontinuities in the rock mass.

3.2. Modification of the experimental velocity expression for a different explosive

Equation (15) is valid only for the rock mass in which the test was conducted and for the explosive that was used during the collection of the velocity and distance measurements. However, this equation can be modified to account for different explosive properties and eliminate the need to conduct additional blasting tests in the given rock mass.

If different explosive properties produce a different value of I, equal to I', then the theoretical particle velocity is

$$u_t' = I' G_t^{-1} \tag{16}$$

Solving for G_t in equation (12) yields:

$$G_t = \frac{I}{u_t} \tag{17}$$

Substituting this expression for G_t into equation (16), the expression for the theoretical velocity, which now applies when an explosive with different properties is used, becomes

$$\acute{u_t} = \frac{\acute{I}}{I} u_t \tag{18}$$

If it is assumed that the field velocities are changed by the same ratio as the theoretical velocities when the explosion term is changed, the equation for field velocity becomes

$$\acute{u_f} = \frac{\acute{I}}{I} I_f {G_t}^{-\alpha} \tag{19}$$

3.3 Modification of the velocity expression to include decoupling

To account for decoupling, one approach is to modify the specific density of the explosive by distributing the weight of the explosive over the volume of the hole.

For example, because the specific density of the explosive is

$$\rho_e = \frac{w_e}{\pi {r_e}^2 L} \tag{20}$$

where w_e is the weight of the explosive and r_e is the radius of the charge, the weight of the explosive can be written as

$$w_e = \rho_e \pi {r_e}^2 L \tag{21}$$

The weight of the explosive per unit volume of the hole is

$$\acute{\rho_e} = \frac{\rho_e \pi {r_e}^2 L}{{r_h}^2 L} \tag{22}$$

where r_h is the radius of the hole.

Simplifying equation (22) yields

$$\acute{\rho_e} = \rho_e \left(\frac{r_e}{r_h}\right)^2 \tag{23}$$

Replacing the specific explosive density term ρ_e in equation (13) by the modified expression ρ_e given by equation (23) and simplifying yields

$$= \frac{r_e}{r_h} \sqrt{\frac{\rho_e q_e}{8\rho_r}} \tag{24}$$

Equation (24) implies that decoupling will reduce particle velocity by the ratio r_e/r_h.

4. FIELD TESTS

4.1 Background

Two series of single-charge tests and a series of drift round tests were conducted in magnetite ore on the 792 m level at the southern end of the Kiruna Mine by researchers from SveBeFo and LKAB. A plan view of the overall test arrangement is shown in Figure 2. Particle velocity measurements for the single-charge test analyzed in this study, called Zero Test 2, and the drift rounds were measured using accelerometers installed in holes drilled from Drift 408 toward Drift 406. The acceleration signals were logged and then integrated to obtain PPV values. The first maximum PPV value in the wave train was used based on findings by Bjarnholt and Skalare (Bjarnholt and Skalare 1981). Saw cuts were made in the ribs of the Drift 406 at several locations after blasting the drift rounds to assess the extent of rock damage. The overall objective was to relate the PPV to the damage distance from the contour charge.

In this paper, velocity and distance measurements from Zero Test 2 along with theoretical PPVs calculated using Neiman's equations are used to determine a damage range caused by a single charge. The relationships developed based on the data collected from Zero Test 2 are then used to analyze the damage caused by the stoping, easer, and perimeter holes in two of the drift rounds.

4.2 Zero Test 2

Zero Test 2 consisted of single charges detonated individually in 5-m-long holes drilled into the face of Drift 406 as shown in Figures 3 and 4. All together, 12 single-shot charges were detonated. Of these, only 5 produced usable results because the particle velocities produced by primer or detonating cord charges used in some of the blasts were too small to measure. In this paper, the focus is on the results obtained with blasting fully-coupled charges (Holes 1, 2, and 3) containing the repumpable emulsion explosive Kimulux R. Blasthole 1 had a diameter of 100 mm, blasthole 2 a diameter of 76 mm and blasthole 3 a diameter of 64 mm. The three holes were shot sequentially in different blasts beginning with hole 1. The bottom end of each of the charges in holes 1, 2, and 3 was approximately 2 m from the bottom of the blastholes. Blast initiation was at the end of the charge. Blastholes 4 and 5 were used for single-shot decoupled charges. The explosive, blasthole diameter, charge diameter, and charge length used are listed in Table II. The explosive properties are listed in Table III.

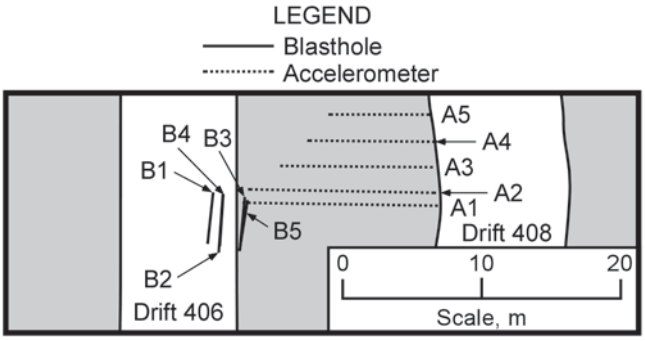

Figure 3- Plan view of Zero Test 2.

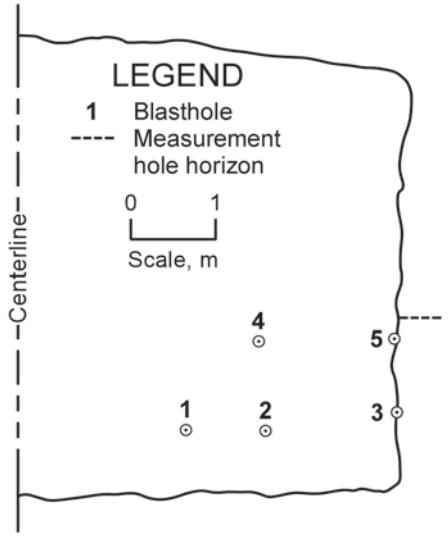

Figure 4- Elevation view of Zero Test 2 at Drift 406 face.

The measurement holes were drilled perpendicular to the blast holes from Drift 408 and were located approximately in the same plane as the blastholes. Three-directional accelerometer readings were recorded in the measurement hole closest to the blastholes; otherwise, the measurements were bidirectional.

Blasthole	Shot	Explosive	Blasthole diameter (mm)	Charge diameter (mm)	Charge length (m)
1	1	KR[a]	100	100	0.480
2	1	KR	76	76	0.490
3	1	KR	64	64	1.100
4	1	K42[b]	48	22	0.682
4	2	K42	48	22	0.682
5	1	K42	48	22	0.682
5	2	K42	48	22	0.682

[a]Kimulux R
[b]Kimulux 42

Table II- Explosive, blasthole diameter, and charge geometry for Zero Test 2 (Nyberg et al. 1998)

Explosive	Kimulux R	Kimulux 42
Weight strength (%)	81	90
Volume strength (%)	115	114
Density (kg/m^3)	1,200	1,100
Velocity of detonation (m/s)	5,500	5,000
Gas volume (l/kg)	906	874
Energy (MJ/kg)	2.94	3.35
Detonation pressure (GPa)	9.1	6.8

Table III- Explosive properties (Nyberg et al. 1998)

The results from the fully coupled charge (shots 1-3) tests

- distance from the charge
- measured PPV
- theoretical PPV using equations (1-11)

are listed in Table IV. The three-dimensional equations for PPV were used because the accelerometers were not located exactly on the x axis of the charges which is required for equation (12).

Blasthole	Distance (m)	Measured PPV (m/s)	Theoretical PPV (m/s)
1	2.89	1.03	0.82
1	3.86	0.69	0.46
1	6.98	0.19	0.14
1	9.75	0.10	0.07
1	12.19	0.02	0.05
2	2.28	0.22	0.95
2	3.35	0.15	0.44
2	5.73	0.07	0.15
2	9.21	0.02	0.06
2	11.8	0.01	0.04
3	2.19	0.26	1.76
3	3.14	0.99	0.84
3	5.81	0.24	0.24
3	8.57	0.12	0.11
3	9.30	0.05	0.09

Table IV- Distance from charge center to accelerometer, measured PPV, and theoretical PPV for Zero Test 2.

For blasthole 1, an examination of the PPV values in Figure 5 reveals the measured PPVs are 31% larger than the theoretical PPVs. For blasthole 2, the measured PPVs are 55% of the theoretical PPVs. For blasthole 3, the result obtained at the 2.19 m distance appears to be an outlier. The four other readings were 23% larger than the theoretical PPVs. The larger values of PPV were unexpected for the field results compared to theoretically calculated PPVs using the three-dimensional equations for blastholes 1 and 3 because the rock mass is quite jointed. Others, however, have reported similar results (Arbiev 1964, Zaitsev 1968, Tseitlin & Smolin 1972). The conclusions from the Kiruna data are:

- Because PPV's from blasthole 1 were measured in virgin rock and blasthole 3 results were only 8% less than those from blasthole 1, blasthole 3 had little damage from either blasthole 1 or blasthole 2. Thus, based on blasthole spacing shown in Figure 4 for blasthole 1, the damage extent was greater than 0.9 m but less than 2.5 m.
- For blasthole 2, which was damaged, the damage range was less than 1.6 m.
- Because the measured PPVs for blasthole 1 were 31% larger than the theoretical PPVs calculated using the theoretical three-dimensional, hydrodynamic-based equations, the expected PPVs in Kiruna virgin rock can be calculated using the theoretical three-dimensional equations and then multiplied by 1.31.
- Equation (12), which is a simplification of the theoretical three-dimensional equations, can be modified to calculate expected PPVs in Kiruna virgin rock along the x axis as shown in Figure 1 by multiplying the results by 1.31.

A range for the critical PPV for the Kiruna rock mass is then calculated as follows. The parameter I is first determined by substituting the density of the explosive, the specific energy of the explosive, and the density of the rock into equation (13). The result is

$$I = 303$$

The theoretical radial velocity is then computed using equation (12) as follows:

$$u_t = 303 G_t^{-1} \tag{25}$$

Applying the calibration factor for the Kiruna rock mass, equation (15) becomes

$$u_f = 397 G_t^{-1} \tag{26}$$

The charge geometry for blasthole 1 is then used to calculate the critical PPV range because the assessed damage was caused by this charge. Substituting

$L = 0.48$ m,
$d = 0.1$ m,
$r = 0.9$ m,

into equation (14), one finds that

$G_t = 37.$

In turn, equation (26) yields 10.7 m/s for the critical PPV (u_t). Similarly, if a value of 2.5 m for r is substituted into equation (14), G_t is computed as 279 and the critical PPV is then equal to 1.4 m/s. The critical PPV range is then 1.4 m/s < PPV_{limit} < 10.7 m/s. As a comparison, the limiting PPV based on the unconfined compressive strength of the rock mass is

$$PPV_{limit} = \frac{\sigma_c}{\rho_r c} = 4.9 m/s \tag{27}$$

where
σ_c = unconfined compressive strength of the rock mass, MPa
ρ_r = specific density of the rock mass, kg/m^3
c = seismic velocity of the rock mass, m/s.

Equation (26) in expanded form is

$$u_f = 397 \frac{\sqrt{v_s}\frac{r}{d}\sqrt{\frac{r^2}{d^2}+\frac{\frac{L^2}{d^2}}{4}}}{\frac{L}{d}} \tag{28}$$

If 4.9 m/s is used in equation (28), the expected damage distance, r, is 1.3 m.

4.3 Measurements conducted during drift driving

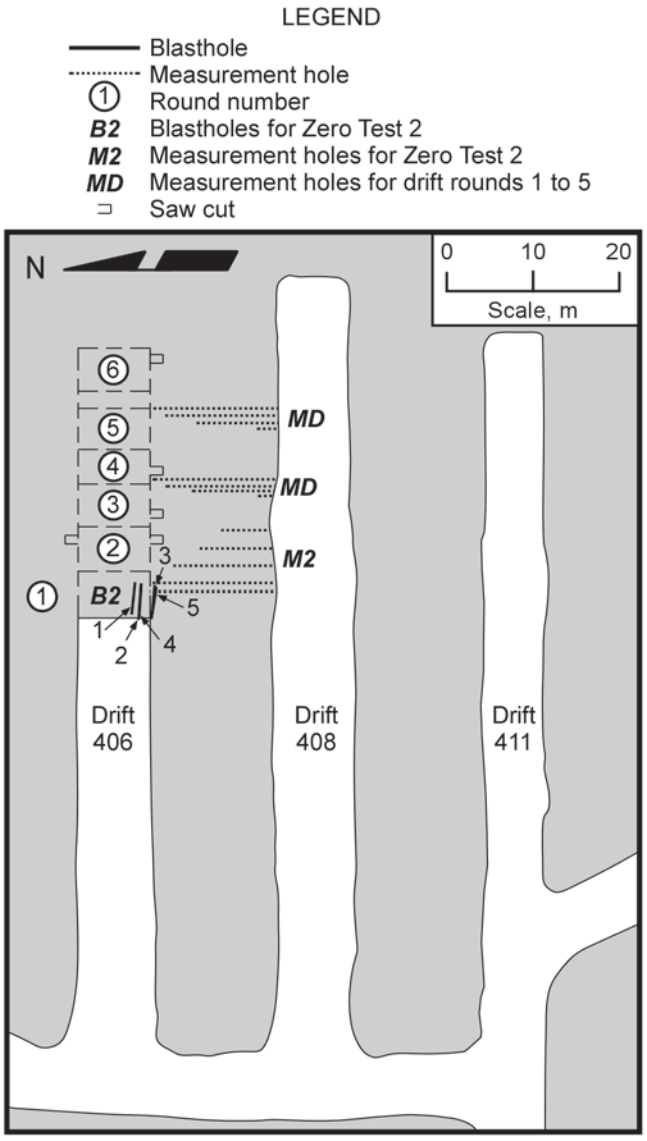

Figure 2- Plan view of Kiruna Mine test arrangement

As part of the test series, a total of six drift rounds were blasted in the orebody of the Kiruna Mine to collect particle velocity measurements at various distances (Jinnerot & Nilsson 1998). Each drift had a cross sectional area of about 42 m^2 and the nominal advance was 5 m. All holes were 48 mm in diameter. The charge length was 4.6 m. No stemming was used. Of the six rounds, only data from rounds 3 and 5 were analyzed because drilling precision on the other rounds was low or accelerometers malfunctioned. Blasthole locations for these two rounds are provided in Figures 6-9. Accelerometers were installed in measurement blastholes that were drilled perpendicular to test Drift 406 from the adjacent parallel Drift 408 as shown in Figure 2. Kimulux R explosive was pumped into the stoping and easer/helper holes and, hence, the explosive was fully

coupled. The contour holes, on the other hand, were charged with 22-mm-diameter, Kimulux 42 cartridges which were decoupled. The peak particle velocity measurement, distance from the center of each charge to each accelerometer, and calculated PPVs using equations 1 through 11 are listed in Tables V and VI for rounds 3 and 5, respectively.

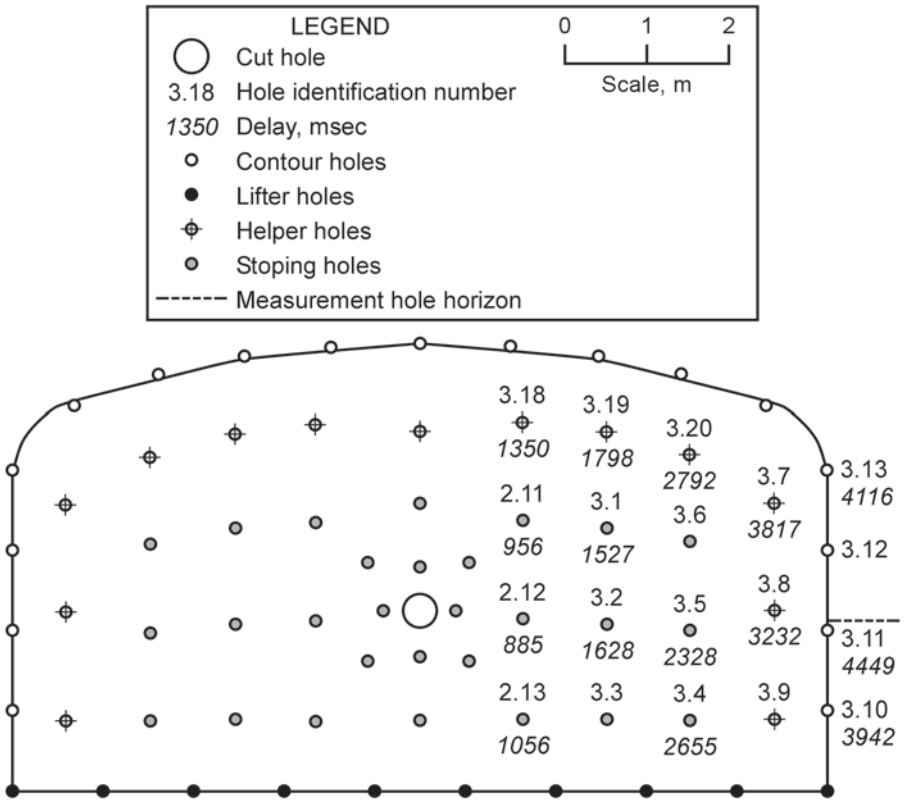

Figure 6- Blast pattern for drift round 3

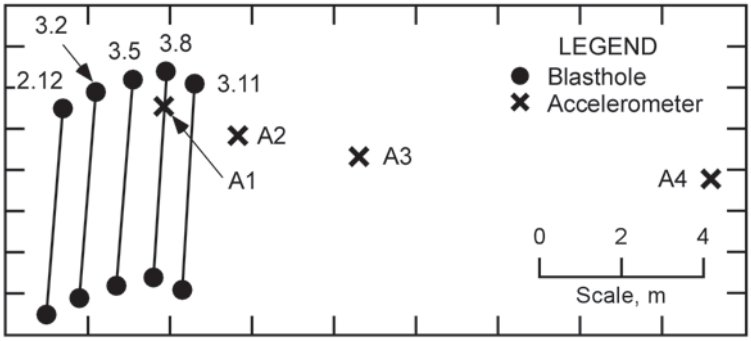

Figure 7- Plan view of blastholes and accelerometers for Drift 3 on approximately the same horizon.

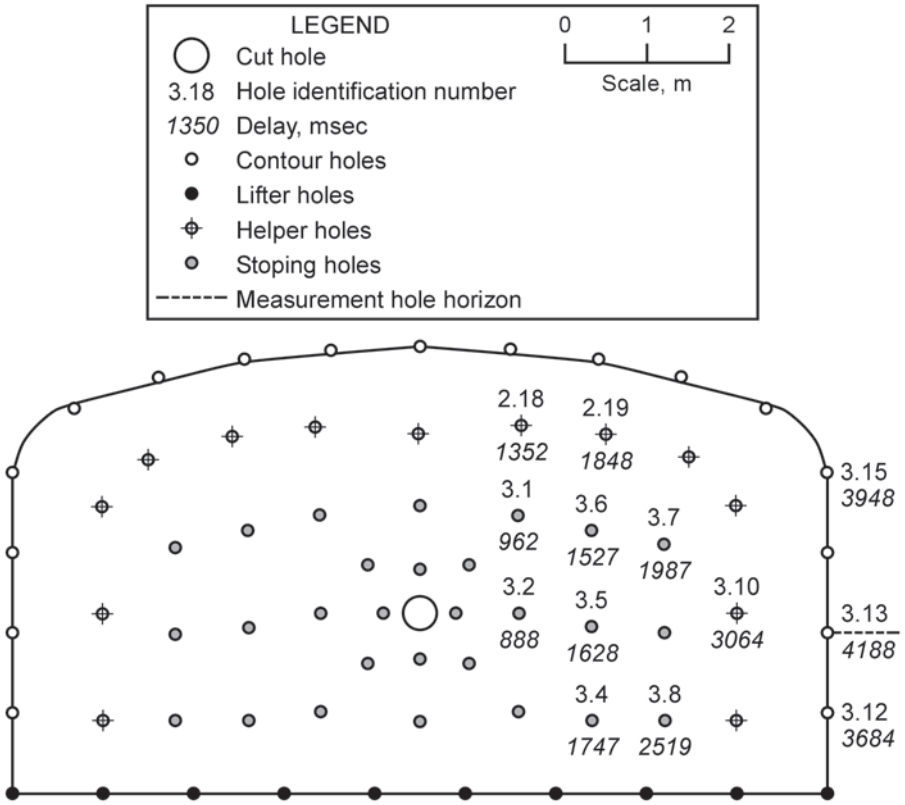

Figure 8- Blast pattern for drift round 5.

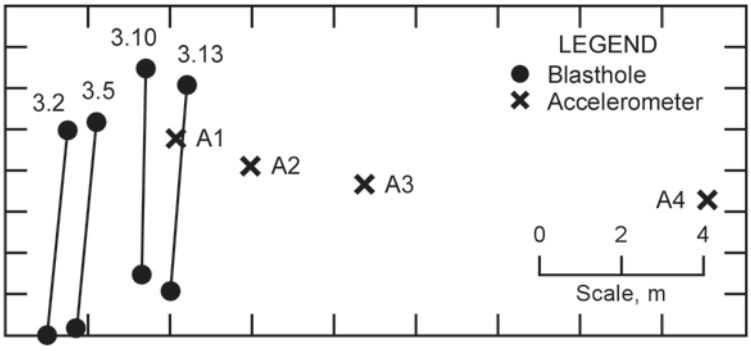

Figure 9- Plan view of blastholes and accelerometers for Drift 5 on approximately the same horizon.

Blasthole	**Accelerometer**	**Distance[a] (m)**	**Measured PPV (m/s)**	**Calculated[b] (m/s)**
3.7	2	3.0	0.959	2.433
3.7	3	5.46	0.262	0.809
3.8	3	4.86	0.327	0.791

2.11	1	3.32	0.438	1.671
2.11	2	4.68	0.274	0.845
2.11	3	7.5	0.114	0.351
2.12	3	7.47	0.113	0.356
2.12	4	15.92	0.021	0.080
2.13	3	7.47	0.135	0.350
2.13	4	16.02	0.025	0.079
3.1	1	2.5	0.803	2.583
3.1	2	3.8	0.465	1.221
3.1	3	6.63	0.182	0.444
3.1	4	15.09	0.038	0.090
3.2	3	6.63	0.11	0.444
3.2	4	15.13	0.021	0.089
3.4	2	2.8	0.514	2.059
3.4	3	5.72	0.126	0.589
3.4	4	14.25	0.022	0.101
3.5	3	5.7	0.122	0.588
3.18	1	4.06	0.525	1.164
3.18	2	5.55	0.306	0.745
3.18	3	8.24	0.193	0.363
3.18	4	16.39	0.028	0.087
3.19	1	3.53	0.519	1.534
3.19	2	4.89	0.314	0.990
3.19	3	7.5	0.225	0.453
3.19	4	15.6	0.038	0.098
3.20	1	2.67	0.639	2.313
3.20	2	3.79	0.418	1.415
3.20	3	6.36	0.222	0.562
3.20	4	14.5	0.039	0.106
3.10[c]	2	1.47	1.168	NA
3.10 [c]	3	4.34	0.105	NA
3.11 [c]	1	1.81	0.711	NA
3.11 [c]	2	1.1	0.501	NA
3.12 [c]	2	1.77	0.314	NA
3.12 [c]	3	4.39	0.070	NA
3.13 [c]	1	2.92	0.101	NA
3.13 [c]	2	2.55	0.100	NA

[a]Distance from center of charge to accelerometer
[b]Calculated using equation 11
[c]Decoupled

Table V- Measured distance from charge, measured PPV, and calculated PPV for round 3.

Blasthole	**Accelerometer**	**Distance[a] (m)**	**Measured PPV (m/s)**	**Calculated[b] PPV(m/s)**

3.10	2	2.49	0.708	2.444
3.10	4	13.6	0.025	0.110
2.18	2	5.04	0.493	0.742
2.19	2	4.55	0.392	1.077
2.19	3	7.07	0.167	0.477
2.19	4	15.09	0.051	0.099
3.1	1	3.34	0.845	1.749
3.1	2	4.89	0.524	0.792
3.1	3	7.58	0.218	0.344
3.2	2	4.9	0.536	0.825
3.4	1	2.62	0.478	2.265
3.4	2	4.26	0.452	1.002
3.4	3	7.0	0.202	0.402
3.4	4	15.25	0.045	0.088
3.5	1	2.53	0.987	2.688
3.5	2	4.04	0.656	1.100
3.5	3	6.78	0.259	0.425
3.5	4	15.11	0.056	0.089
3.6	1	2.9	1.244	3.219
3.6	2	4.12	0.802	1.121
3.6	3	6.71	0.338	0.435
3.6	4	14.98	0.073	0.091
3.7	1	2.45	1.570	5.588
3.7	2	3.47	1.156	1.558
3.7	3	6.01	0.441	0.535
3.8	1	2.67	1.334	2.953
3.8	2	4.21	1.241	1.337
3.8	3	6.76	0.542	0.596
3.8	4	14.27	0.112	0.110
3.12[c]	1	.87	1.529	NA
3.12 [c]	3	4.65	0.232	NA
3.12 [c]	4	12.87	0.044	NA
3.13 [c]	2	1.26	0.292	NA
3.13 [c]	3	4.5	0.073	NA
3.13 [c]	4	12.84	0.014	NA
3.15 [c]	1	2.1	1.070	NA
3.15 [c]	2	3.07	0.390	NA
3.15 [c]	3	5.25	0.146	NA
3.15 [c]	4	13.11	0.038	NA

[a]Distance from center of charge to accelerometer
[b]Calculated using equation (11)
[c]Decoupled

Table VI- Measured distance from charge, measured PPV, and calculated PPV for round 5.

5. ANALYSIS OF BLAST DAMAGE IN THE DRIFT ROUNDS

The damage range for a fully coupled charge of Kimulux R in the 48-mm diameter holes (stoping and easer/buffer) can be calculated using equation (28). For the limiting critical PPV values (PPV_{min} = 1.4 m/s and PPV_{max} = 10.7 m/s) obtained in Zero Test 2, the corresponding values of G_t are 281.4 and 37.2, respectively. Beginning with PPV_{min}, substituting G_t equals 281.4 together with the required charge dimensions into equation (28), r equals 85.5.

For a blasthole diameter of 48 mm, the maximum predicted damage radius (r) would be 4.1 m. Applying the same procedure for PPV_{max} equal to 10.7 m/s, the predicted damage radius equals 1 m which is considered to be a more reasonable value. The damage range for a single fully coupled hole is then 1 m to 4.1 m.

Theoretical velocities using equations 1 through 11 are compared to measured velocities for fully coupled rounds 3 and 5 in Tables V and VI. Some holes are located approximately on the same elevation as accelerometers 3 and 4, which are positioned close to a line perpendicular to the centroid of each round. These conditions justify the application of equation 25 to calculate PPV. A charge length equal to 4.6 m and a blasthole diameter equal to 0.048 m are used to calculate G_t for the chosen distances. These values are then substituted into equation (26). The results are listed in Table VII and plotted in Figure 10. As shown in Tables V through VII and Figure 10, the measured PPVs are much less than the calculated PPVs. This indicates that blast damage occurred around each charge prior to detonation. This observation is in agreement with that made by Blair (Blair & Armstrong 2001). The damage distance is at least equal to the blasthole spacing of about 1 m which is compatible with the calculated damage range based on PPV_{max}. If the calculated PPV values from Table VII are reduced by using the regression equation for blasthole 3 shown in Figure 5, the calculated PPV's are closer to the measured PPVs. The reduced PPV values are plotted in Figure 10. This is another indication that the rock around blastholes in rounds 3 and 5 was damaged prior to detonation.

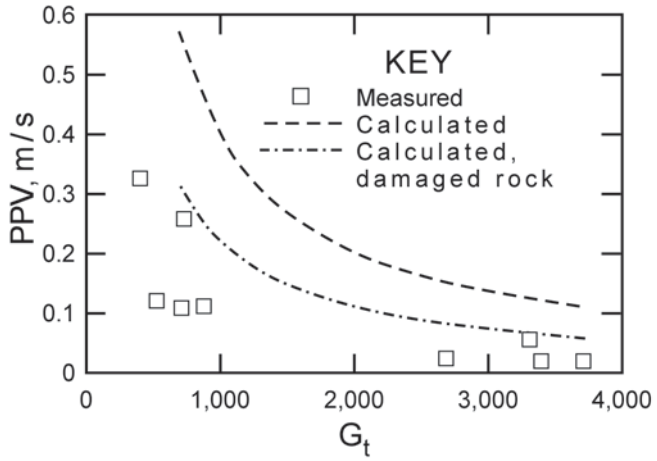

Figure 10- PPV versus G_t for coupled charges, rounds 3 and 5.

Round	Blasthole	Accelerometer	Distance [a] (m)	Measured PPV (m/s)	G_t	Calculated [b] PPV (m/s)
3	2.12 (E)[c]	3	7.5	0.113	864	0.46
3	2.12 (S)[d]	4	15.8	0.021	3760	0.11
3	3.2 (S)	3	6.7	0.11	697	0.57
3	3.2 (S)	4	15.1	0.021	3387	0.12
3	3.5 (S)	3	5.7	0.122	514	0.77
3	3.8 (E)	3	4.9	0.327	389	1.01
5	3.5 (S)	3	6.8	0.259	717	0.55
5	3.5 (S)	4	14.9	0.056	3299	0.12
5	3.10 (E)	4	13.4	0.025	2675	0.15

[a]Distance from center of charge to accelerometer
[b]Calculated using equation (26)
[c]Easer hole
[d]Stoping hole

Table VII- Measured and calculated PPV for coupled charges, Rounds 3 and 5.

The expected PPV values from the contour rounds can be calculated by applying modifying factors to equation (26). The explosive parameter, I, for Kimulux 42 which was used in the contour rounds is I equals 310. Dividing by I equals 303, the explosive parameter for Kimulux R used for Zero Test 2, one obtains

$$\frac{I'}{I} = \frac{310}{303} = 1.023$$

The decoupling factor (r_e/r_h) is 0.458. Applying these factors to equation (26) yields

$$u_f = 186 {G_t}^{-1} \qquad (29)$$

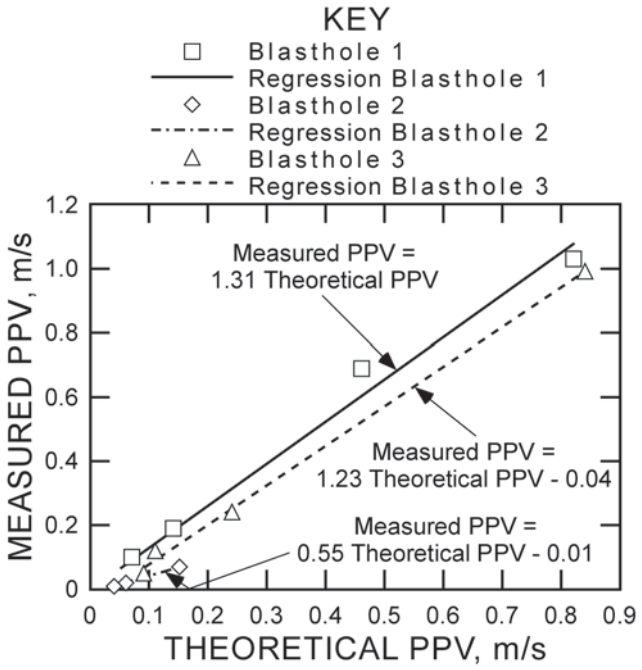

Figure 5- Measured versus theoretical PPV for blastholes 1-3.

As shown in Table VIII, the measured PPV values from the decoupled holes located on the measurement hole horizon are much less than the PPV values as calculated from the Zero Test 2 results. This indicates that the charges in the buffer/easer/helper holes likely caused damage in the rock mass containing the contour hole. As a result of this damage, the particle velocity carried by the p-wave from the contour charge is presumed to have been strongly attenuated. This is consistent with observations by Jinnerot and Nilsson (1998) who could not confirm visible perimeter damage in 1.5-m by 1.0-m saw cuts made in the drift walls after excavation. The observations, however, were hampered by the presence of the natural jointing and joint variability. They further state that the cracks that one sees are probably natural cracks with a variation which is geologically based. If the calculated PPV values from Table VIII are reduced by using the regression equation for blasthole 2 shown in Figure 5, the calculated PPVs are closer to the measured PPVs but still larger. This reflects the severity of damage around the decoupled blastholes. The reduced PPVs are listed in Table VIII.

Round	**Blasthole**	**Accelerometer**	**Distance[a] (m)**	**Measured PPV (m/s)**	**G_t**	**Calculated PPV (m/s)**	
3	3.11	2	1.8	0.501	77	2.4[b]	1.31[c]
5	3.13	2	2.0	0.292	90	2.1	1.15
5	3.13	3	4.6	0.073	347	0.54	0.29
5	3.13	4	12.7	0.014	2407	0.08	0.03

[a]Distance from center of charge to accelerometer
[b]Calculated using equation (26)
[c]Calculated using equation (26) modified for damaged rock

Table VIII- Measured and calculated PPV for decoupled charges, rounds 3 and 5.

6. APPROACH TO CONTROLLED BLASTING

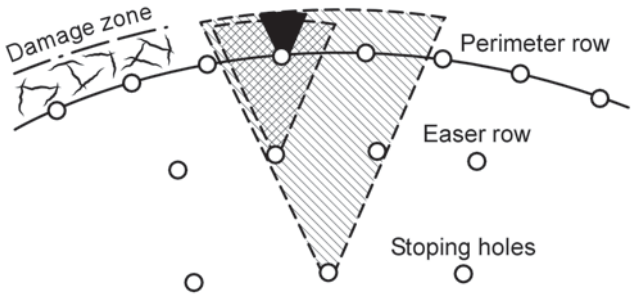

Figure 11- Coinciding damage limits (after Holmberg 1982).

Figure 11 (Holmberg 1982) is a diagrammatic representation of the contour control blast design principle behind the Holmberg (1982) approach. One begins with the design of the contour row and selects the charge concentration and hole spacing based on the allowable damage limit. Knowing the location of the maximum damage limit outside of the perimeter, one selects the explosive charge and the easer hole location so that the damage limit from the easer row does not exceed that of the contour row. The same procedure is followed for the stoping row of holes. The design curves provided by Holmberg & Persson (1978, 1979) relating PPV to the distance as a function of the linear charge concentration is often applied for this purpose (see Figure 12). This design approach assumes that the same set of curves applies for each of the different holes. However, it does not take into account the fact that in practical application the charges are detonated in the opposite order from that of the design. The stoping holes are blasted first, followed by the easer row, and finally the contour row is shot. Depending on the charging and proximity of the holes to one another, various degrees of damage are induced to the adjacent rock mass before the given explosive detonates. For example, if the limiting PPV is 1,000 mm/s, then the damage distance in fresh rock for a charge concentration of 1.5 kg/m is about 1.4 m as shown in Figure 12. If the rock is predamaged, then the actual contour line would lie below the design curve. For illustrative purposes, if this line coincides with the 0.5 kg/m contour line based on virgin rock conditions, then the damage for the same charge concentration of 1.5 kg/m is only 0.7 m.

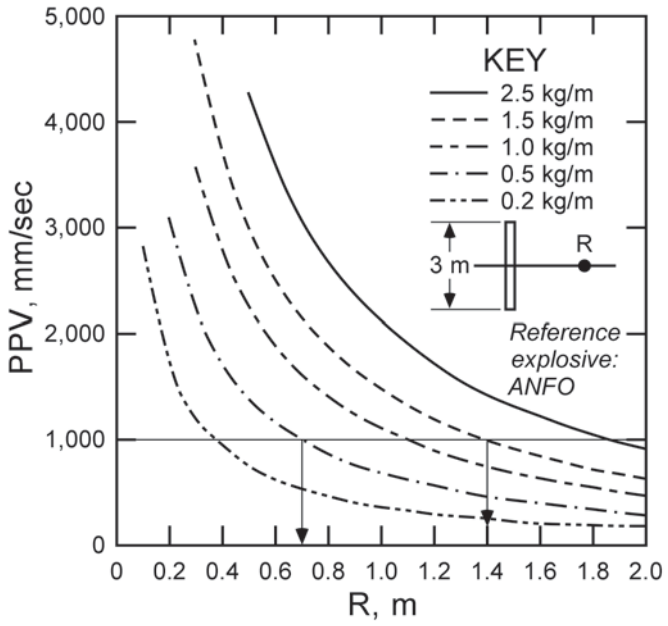

Figure 12- Peak particle velocity as a function of distance and charge concentration for a 3-m-long charge (after Holmberg & Persson 1979).

The results reported in this paper show that the predamage can be significant and the peak particle velocities are expected to be less, in fact much less, than might be predicted using theoretical curves such as given in Figure 12. This suggests that the perimeter design approach is conservative. These results also help to explain why the extent of damage from fully coupled perimeter holes is often less than might be predicted. In this case, some damage to the rock containing the contour holes has probably been done by the easer row of holes and a more rapid attenuation of the damage producing waves occurs than would normally be the case.

The effect of pre-damaged rock and associated wave attenuation on damage distance is also demonstrated by examining the results of Zero Test 2. Figure 13 is a plot of PPV versus scaled distance. The limiting PPV as defined by Equation (27) is equal to 4.9 m/s for the Kiruna rockmass. The scaled damage distance for blasthole 1, which was located in intact rock is 0.8 $m/kg^{0.5}$ and the scaled damage distance for blasthole 2, which was located in damaged rock is 0.3 $m/kg^{0.5}$. Using charge geometry from Table 2 and charge density from Table 3, the damage distances for blastholes 1 and 2 are 1.7 m and 0.5 m, respectively.

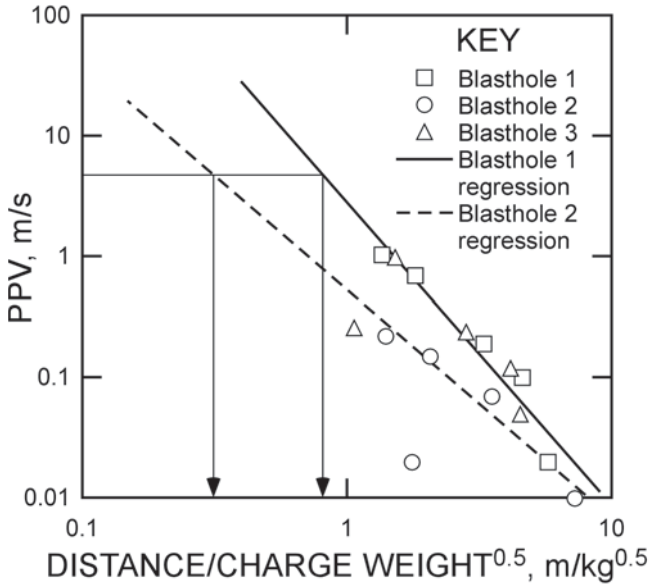

Figure 13- Peak particle velocity versus scaled distance for Zero Test 2.

7. CONCLUSION

Velocity and distance measurements from a series of single-shot tests performed by Swedish researchers at the Kiruna Mine, together with equations based on hydrodynamics, were used to develop PPV versus distance data for undamaged rock. Based upon knowing the charge distances at which damage was present or absent, it was possible to bracket the critical peak particle velocity. In this case, the PPV range was quite large ranging from 1.4 m/s to 10.7 m/s. In the future, some special observation techniques, such as the visual inspection of rock damage from a saw cut into the rib after a single blast, could provide a smaller range for the critical PPV. In this regard, Olsson (Olsson et al. 2009) have recently presented 3D fracturing results from a very complete set of such saw cuts in granite.

The equation developed from the single-charge tests was then used to calculate the expected PPV values at various known distances from drift round charges with different geometry than the charges used in the single-charge test. A comparison between calculated and measured PPV values for the stoping, easer, and contour holes indicate that, in all cases, there was some apparent predamage to the rock surrounding the charges prior to their detonation. The result was that the measured PPV values were significantly less than would be predicted based on tests conducted in undamaged rock.

The findings are highly significant and positive in that designs based on the use of PPV versus distance curves obtained in fresh rock will be conservative, perhaps quite conservative. The actual damage extent is expected to be less than predicted and designed. In this situation, the waves emanating from even a fully coupled perimeter charge could be rapidly attenuated if the hole was in the influence zone of the easer hole

row. This could account for the fact that sometimes the overbreak associated with fully coupled perimeter charges is less than anticipated.

This excellent set of data produced by LKAB and SveBeFo has offered an opportunity to apply an analysis technique based on hydrodynamics and to gain an insight into the complicated blast damage process. The data have been included so that others might apply their own analysis techniques. In particular, the effect of end initiation as opposed to instantaneous detonation, which is assumed in the Neiman approach, could be addressed.

ACKNOWLEDGEMENT

The authors wish to thank Sten Fernerud, Fenerud Engineering AB, Umeå, Sweden, and Anders Nordqvist, LKAB, Kiruna, Sweden, for providing information on Zero Test 2.

REFERENCES

(1) Arbiev, K. K. (1964) Investigation of the effectiveness of use of blast holes of various dimensions in relation to the physicomechanical properties and temperature regime of the rocks in quarries in the Norilsk Combine. PhD Thesis, Leningrad.

(2) Bjarnholt G & H. Skalare (1981) Instrumented rock blasting – Initial test in a concrete block. Sve Be Fo Report DS 1981:16, Stockholm. (In Sewdish)

(3) Blair, D.P. & L.W. Armstrong (2001) The influence of burden on blast vibration. *The International Journal for Blasting and Fragmentation 5*(1-2):108-129.

(4) Blair, D.P. (2008) Non-linear superposition models of blast vibration. *International Journal of Rock Mechanics and Mining Sciencesp45*(2):235-247.

(5) Blair, D.P. & A. Minchinton (2006) Near-field blast vibration models. In: *Proceedings of the 8th International Symposium on Rock Fragmentation by Blasting*, Asociación Chilena de Ingenieros Explosivistas de Chile A.G. (ASIEX), pp. 152-159, Santiago.

(6) Holmberg R. (1982) Charge calculations for tunneling. *Underground Mining Methods Handbook*, Soc. of Mining Engineers of AIME (Ed.: W.A. Hustrulid), NY, pp. 1580-1589.

(7) Holmberg, R. & P.A. Persson (1978) The Swedish approach to contour blasting. In: *Proceedings of the 4th Conference on Explosives and Blasting Technique,* New Orleans, February 1-3, ISEE, pp. 113-127.

(8) Holmberg, R. & P.A. Persson (1979) Design of tunnel perimeter blasthole patterns to prevent rock damage. In: *Proceedings, Tunnel* '79. (Ed.: M.J. Jones), pp. 280-283, IMM, London.

(9) Hustrulid, W. (1999) *Blasting Principles for Open Pit Mining Volume 2 – Theoretical foundations*. Balkema, Rotterdam.

(10) Hustrulid, W. et al. (1992) A New Method for Predicting the Extension of the Blast Damaged Zone. In: *Proceedings of the Blasting Conference*, Nitro Nobel, January 15–16.

(11) Iverson, S.R. et al. (2009) The extent of blast damage from a fully coupled explosive charge. In: 9th *International Symposium on Rock Fragmentation by Blasting*. (Ed.: Sanchidrián), pp. 459-468, Taylor & Francis Group, London.

(12) Jinnerot, M. & H. Nilsson (1998) Experimental study of shock wave propagation and damage zone calculation during drift driving. Senior Thesis, Chalmers Technical University, Gothenberg, Sweden,

(13) Lizotte, Y.C. (1994) Controlled blasting experiments in a small drift at the CANMET experimental mine. CANMET-MRL 94-014(TR), pp. 15-20.

(14) Lupo, J.F. (1997) Progressive failure of hanging wall and footwall Kiirunavaara Mine, Sweden. *International Journal of Rock Mechanics and Mining Sciences 34*:3-4, paper No. 184.

(15) Miller, H. & T.W. Camm (2009) An economic analysis of controlled drilling & blasting techniques in underground drift development. National Institute for Occupational Safety and Health (NIOSH) internal report.

(16) Neiman, I.B. (1976) Determination of the dimensions of the crushing in bounded rock massif due to the explosion of a cylindrical loosening charge. PhD. Thesis, Novosibirsk.

(17) Neiman, I.B. (1979) Determination of the zone of crushing of rock in place by blasting. *Soviet Mining Science 15*(5): 480-485.

(18) Neiman, I.B. (1984a) Mathematical model of the explosive action of a fracturing charge in a ledge of rock mass. *Soviet Mining Science 19*(6): 494-499.

(19) Neiman, I.B. (1984b) Correction of the hole charge parameters in rock bench breaking. *Soviet Mining Science 20*(5): 385-388.

(20) Neiman, I.B. (1986a) Modeling the explosion of a system of borehole charges in a scarp. *Soviet Mining Science 22*(2): 108-113.

(21) Neiman, I.B. (1986b) Volume methods of the action of a cylindrical-charge explosion in rock. *Soviet Mining Science 22*(6): 455-462.

(22) Nyberg, U. (1998) Study of the damage zone in magnetite ore from blasted drifts. Initial study of de-coupled single charges. Progress Report 1 for SveBeFo Project 637, July 14, 1998.

(23) Nyberg, U. et al. (1998) The judgment of blast damage at the drift contour: vibration measurements, damage prediction and crack mapping in magnetite ore and waste. Sve Be Fo Report 50.

(24) Olofsson, S.O. (1990) *Ap lied explosives technology for construction and mining*. Applex AB, Ärla, Sweden, pp. 206-221.

(25) Olsson, M. et al. (2009) Examination of the excavation damage zone in the TASS tunnel, Äspo HRL. SKB Report R-09-39.

(26) Tseitlin, Y.I. & N.I. Smolin (1972) Effect of blasting on the rock foundation of hydraulic structures. *Hydrotechnical Construction 6(7)*:650-656.

(27) www.LKAB.com retrieved on 2/20/2010.

(28) Zaitsev, M.M. (1968) Investigation of the effectiveness of breaking down hard ledge rocks by paired blast hole charges in quarries of the Norilsk combine. Ph.D. Thesis, Leningrad.